Monitoring anthracycline cancer drug-nucleosome interaction by NMR using a specific isotope labeling approach for nucleosomal DNA

Emmerik, C.L. van; Lobbia, V.; Neefjes, J.; Nelissen, F.H.T.; Ingen, H. van

ChemBioChem

Research Article
doi.org/10.1002/cbic.202400111

Chemistry Europe
European Chemical Societies Publishing

www.chembiochem.org

Monitoring Anthracycline Cancer Drug-Nucleosome Interaction by NMR Using a Specific Isotope Labeling Approach for Nucleosomal DNA

Clara L. van Emmerik,[a] Vincenzo Lobbia,[a] Jacques Neefjes,[b] Frank H. T. Nelissen,[c] and Hugo van Ingen*[a]

Chromatinized DNA is targeted by proteins and small molecules to regulate chromatin function. For example, anthracycline cancer drugs evict nucleosomes in a mechanism that is still poorly understood. We here developed a flexible method for specific isotope labeling of nucleosomal DNA enabling NMR studies of such nucleosome interactions. We describe the synthesis of segmental one-strand ^{13}C-thymidine labeled 601-DNA, the assignment of the methyl signals, and demonstrate its use to observe site-specific binding to the nucleosome by aclarubicin, an anthracycline cancer drug that intercalates into the DNA minor grooves. Our results highlight intrinsic conformational heterogeneity in the 601 DNA sequence and show that aclarubicin binds an exposed AT-rich region near the DNA end. Overall, our data point to a model where the drug invades the nucleosome from the terminal ends inward, eventually resulting in histone eviction and nucleosome disruption.

Introduction

In eukaryotes, access to the genetic code is restricted by the wrapping of DNA around the histone proteins in the nucleosome. Modulation of nucleosome dynamics and nucleosome positioning thus plays a crucial role in regulation of chromatin function.[1] The intrinsic dynamics of the nucleosome[2,3] can be altered by epigenetic modifications,[4] binding of proteins,[5,6] as well as small molecules.[7] Over the last decade it has become clear that anthracycline cancer drugs thank their anti-cancer activity at least in part to their disruptive effect on chromatin structure, causing nucleosome eviction from defined regions in the genome, rather than directly causing DNA damage.[8–12] Anthracyclines like doxorubicin are cornerstones in cancer treatment and topoisomerase II poisons. Aclarubicin ('acla') is an anthracycline that only evicts nucleosomes, and is used in the treatment of AML patients.[8] Acla consists of a aglycon moiety, common to other anthracyclines, that intercalates into the DNA and a trisaccharide that has been shown to bind in the minor groove, covering up to 4 base pair steps.[13] Acla prefers poly-AT sequences although sequence specificity is limited.[14,15] Like related anthracyclines such as doxorubucin, acla prefers binding to naked DNA over binding nucleosomes.[16] How anthracyclines such as acla interact with nucleosomes to cause histone eviction is however poorly understood.

To obtain molecular insights in the binding and eviction mechanism requires methodology that allows the site-specific studies of the conformational dynamics of nucleosomal DNA. NMR studies can provide such detailed insight for nucleic acids, so far most clearly demonstrated on RNA.[17–21] Application to the nucleosomal DNA has so far been limited as the size (~200 kDa with histone proteins included) and the length (at least 145 bp[22]) poses significant challenges.

Recently, two different approaches to overcome these challenges have been demonstrated.[23,24] In the study of Abramov *et al.*, nucleosomal DNA was amplified in *E. coli* in perdeuterated form, and after purification ^{1}H,^{13}C-labeled methyl groups were installed on specific cytidine and adenosine bases using recombinant methyltransferases.[23] Exploiting the methyl-TROSY effect for high molecular weight systems,[25] very high quality solution NMR spectra were obtained, affording detailed characterization of DNA dynamics at specific sites in the nucleosome. Yet, there is limited flexibility in the choice of labeled bases as this depends on the specificity of the methyltransferases. In the study of Conroy *et al.* the nucleosomal DNA was uniformly ^{13}C,^{15}N-labeled and interrogated using dynamic nuclear polarization-enhanced solid-sate NMR (DNP-ssNMR).[24] Using minimal amounts of DNA, high quality spectra were obtained to identify the typical signals of each of the four bases, enabling measurement of distances in specific types of

[a] *Dr. C. L. van Emmerik, Dr. V. Lobbia, Dr. H. van Ingen*
NMR Spectroscopy Research Group
Bijvoet Center for Biomolecular Research
Utrecht University
Padualaan 8, 3584 CH Utrecht (The Netherlands)
E-mail: h.vaningen@uu.nl

[b] *Prof. Dr. J. Neefjes*
Cell and Chemical Biology
Leiden University Medical Center
Einthovenweg 20, 2300 RC Leiden (The Netherlands)

[c] *F. H. T. Nelissen*
Biophysical Chemistry
Institute for Molecules and Materials
Radboud University
6525 AJ Nijmegen (The Netherlands)

Supporting information for this article is available on the WWW under https://doi.org/10.1002/cbic.202400111

base pair steps. However, the limited chemical shift dispersion of DNA precluded a site-specific analysis.

Both methods relied on DNA produced in *E. coli* which is only compatible with uniform isotope labeling. Nucleic acids can, however, also be efficiently produced in vitro, offering more flexibility in isotope labeling.[26–28] Here, we detail a flexible strategy for site-specific isotope-labeling of nucleosomal DNA that can be used for both solution and solid-state NMR studies. The method relies on incorporation of tailored, labeled primers in a PCR reaction. It can be tuned to label a specific desired DNA location, specific nucleotides and, possibly, specific spin pairs. As a proof-of-concept, we demonstrate this by the specific labeling of six thymidine nucleotides in the Widom 601[29] strong-positioning DNA. Using a fill-in reaction, a custom primer was produced to subsequently prime a large-scale PCR reaction, resulting in milligram quantities of labeled nucleosomal DNA. With only 6 out of 72 T nucleotides labeled, the methyl-TROSY spectra of the DNA and nucleosomes were of sufficient sensitivity and resolution to resolve their methyl signals. In a 'divide-and-conquer' approach assignments could be transferred from a 15 nucleotide (nt) duplex. The NMR data obtained for the labeled 601 DNA and nucleosome provide evidence for intrinsic conformational flexibility at a key histone-DNA interaction site in the 601 sequence. We further performed a titration of the nucleosomes with aclarubicin, a DNA-intercalating anthracycline cancer drug, showing that aclarubicin binds an exposed AT-rich region near the DNA end. Overall, our data point to a model where the drug invades the nucleosome from the terminal ends inward, eventually resulting in histone eviction.

Results and Discussion

Segmental One-strand Labeling Strategy

Our strategy produces nucleosomal DNA with isotope-labeled nucleotides in one strand at a defined location, as illustrated in Figure 1. First a specifically labeled primer is produced by performing a fill-in reaction using the Klenow fragment of DNA polymerase I in the presence of isotope labeled nucleotides (Figure 1a). The fill-in reaction is performed starting from a template-primer partial duplex with the template having both a 3′ and a 5′ overhang. During the reaction the 5′ overhang is filled-in by the polymerase, while the 3′ overhang remains. This ensures a sufficiently large difference in size of the template and the labeled primer to facilitate separation and purification from a denaturing gel. The lengths of the initial primer and template determine the 5′ and 3′ boundaries, respectively, of the segment that will be isotope-labeled. Therefore, varying these lengths allows tuning of the nucleotides that will be labeled. However, care must be taken to maintain the size difference for the template, initial primer and labeled primer for gel-separation, as this is crucial for purification. Alternatively, the single-strand primer can be purified from a biotinylated template.[30]

The labeled primer is then used to prime a large-scale PCR reaction to produce nucleosomal DNA that can be used for in vitro reconstitution reactions (Figure 1b). Here, we produced a 30 nt primer to label six thymidines at superhelical location (SHL) +6 of a 167 base pair (bp) version of 601-DNA, referred to as 6T-601-DNA below (Figure 1c and Supplementary Scheme S1). Using 145 bp nucleosomal DNA[22] in combination with a primer of up to ~35 nt, nucleotides in the region from SHL ±7 to SHL ±4 can be labeled. The primer cannot be extended much further, as this would decrease efficiency of the PCR reaction. Labeling the central part of the DNA (SHL 0 to ±3) would thus require PCR production of two DNA segments and subsequent ligation.

Production of Labeled Primer, 601-DNA and Nucleosomes

We used a 601-DNA sequence with a total length of 167 bp, including 10 bp of linker DNA on each side. To achieve thymidine isotope-labeling at SHL+6, we used a 38 nt initial template in combination with a 15 nt initial primer, that after fill-in with uniformly ^{15}N- and ^{13}C-labeled dTTP and unlabeled dGTP, dCTP and dATP yielded a 30 nt primer as product, containing six isotope-labeled thymine residues (see Figure 1a and 2). The use of the Klenow fragment for polymerization ensures removal of possible non-templated adenosine residues at the 3′-end of the labeled primer that could cause decreased priming efficiency during PCR. The yield was optimized by

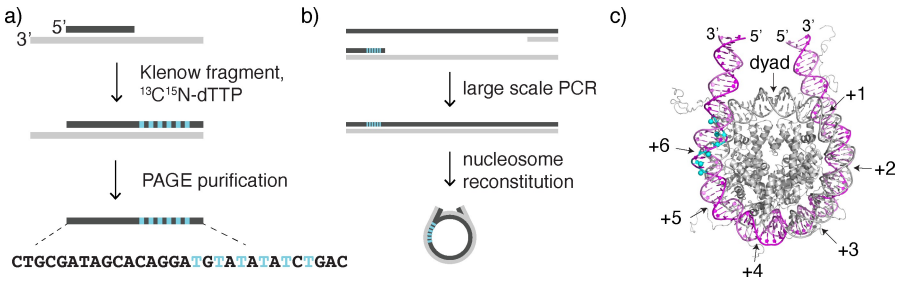

Figure 1. Schematic overview of the synthesis of segmentally isotope-labeled 601-DNA and its incorporation into nucleosomes. (a) An initial primer-template partial duplex is subjected to a fill-in reaction with Klenow fragment in presence of isotope nucleotides. Labeled nucleotides indicated in blue. (b) The labeled PCR primer is used in a large-scale PCR reaction to produce nucleosomal DNA with specifically labeled nucleotides in one strand of the DNA, which is subsequently used to reconstitute nucleosomes. (c) Model of the 167 bp 601-nucleosome with the accessible region for labeling without requiring a ligation step highlighted in magenta/violet and labeled nucleotides in this study in cyan. Numbering of the superhelical locations (SHL) indicated.

varying template-primer ratios (Figure 2). A 1.25-fold excess of initial primer was chosen to limit the amount of left-over primer after the reaction. After gel purification and IEX chromatography, the yield was found to be 6–7 nmol of pure labeled primer per mL of fill-in reaction.

Initially, we attempted to produce the full-length 6T-601-DNA using a second fill-in reaction starting from the labeled primer and stoichiometric amounts of 167-nt ssDNA, produced using rolling circle amplification.[30] Despite several optimization attempts, production of dsDNA was not efficient, likely due to secondary structure formation in the ssDNA template strand. We thus used the segmentally isotope-labeled primer in large-scale PCR to obtain the full-length 601-DNA. To efficiently prepare mg amounts of DNA, we used a 60-well thermoblock that can accommodate 0.5 mL PCR tubes. The PCR tubes contained 200 μL of reaction mixture, and to ensure proper temperature distribution over the whole sample, the time per PCR step was slightly increased. This way, each run (2 hrs) contained 12 mL of PCR reaction and yielded about 0.4 mg product, resulting in the production of 2 mg of purified DNA in 1–2 days (Figure S1).

NMR of the 6T-Labeled DNA and Nucleosome

Before proceeding to use the 6T-labeled DNA for nucleosome reconstitution, we first examined it by NMR, focusing on the signals of the thymine methyl groups that benefit from the methyl-TROSY relaxation interference effect.[25] To assign the methyl resonances, we used a 'divide-and-conquer' strategy, starting from a 15 bp unlabeled DNA duplex. Using homonuclear 2D TOCSY and NOESY, the sequential assignment and thymine methyl assignment could be completed, and the latter transferred to the $^{1}H,^{13}C$-HMQC spectrum (Figures 3a and S2, S3). These assignments were then first transferred to the 6T-labeled product of the Klenow fill-in reaction (Figure 3b). This product contains a 30 bp duplex in which the 6 thymidines are specifically labeled, resulting in a spectral simplification compared to the 15 bp duplex. In the last step these assignments were transferred to the 6T-labeled 167 bp DNA (Figure 3b, see also Figure S3). Notably, the assigned chemical shifts correspond closely to those expected based on the nucleotide sequence, as the observed shifts match the tabulated statistical averages reported by Altona *et al.* .[31] For example, a chemical shift of ~1.6 ppm is expected for thymidines flanked by a pyrimidine at the 5′-end, which is indeed only the case for T27 (CpT, see Figure 3d).

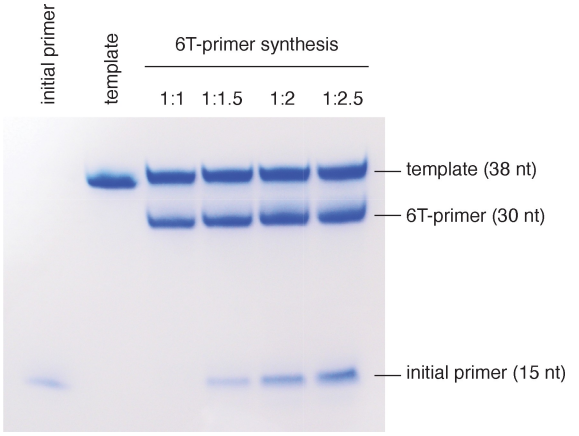

Figure 2. Denaturing PAGE gel of 6T-labeled primer synthesis. Molar ratios of template to initial primer are indicated above each lane.

To obtain high-resolution spectra of the 6T-labeled DNA, constant-time HMQC spectra were recorded at 45 °C to refocus the effect of $^{1}J_{CC}$ couplings and increase the overall molecular tumbling, respectively (Figure 3c). Comparison of the spectra recorded at 10 and 45 °C (see Figure S3 and inset in Figure 3c) revealed significant changes for T27, which gives a single peak at low, and a major and minor peak at high temperature. The T27 methyl resonance also showed high chemical shift variation between the different constructs tested (Figure 3b and Figure S3). These observations are indicative of conformational heterogeneity around T27. Interestingly, T27 is near SHL 5.5 where the minor groove faces the histone octamer (see Figure 3d). The CpA═T27pG dinucleotide step has been highlighted as one of the important points where increased DNA flexibility allows deformation of the minor groove.[32] Thus, our results here illustrate that the conformational flexibility is intrinsic to the nucleotide sequence at SHL 5.5.

Next, we used the 6T-601-DNA to reconstitute nucleosomes (see Figure S1) and recorded the methyl NMR fingerprint again (Figure 3b). Overall, the resonances were somewhat broader compared to the free DNA. Of note, we here used perdeuterated histones to avoid rapid relaxation of the methyl signals by nearby histone protons. Comparison to the free DNA spectrum further showed small chemical shift changes, most clearly for T19 and T25. Intriguingly, T19 and T25 are the only nucleotides that are part of base pairs that form the phosphate binding platforms.[33] At these binding platforms the minor grooves are constrained to fit to histone surface, which can result in base pair step deformations. T19 is part of the platform at SHL 6.5 and T25 at SHL 5.5 (Figure 3d). In addition, the minor T27 peak observed for the free 6T-601-DNA seemed to have disappeared, or at least have lower relative intensity compared to the main peak, suggesting that the DNA conformation is stabilized inside the nucleosome. While the sample likely contains a small percentage of free DNA, the observed changes in line width and peak pattern compared to the free 6T-labeled DNA spectrum indicate that the observed signals originate from DNA in the nucleosome. Together, the results on 6T-labeled DNA and the 6T-labeled nucleosomes demonstrate the specific labeling approach taken here can generate high-resolution spectra to probe conformational dynamics of nucleosomal DNA at atomic resolution.

Interaction with Aclarubicin

To explore the feasibility of our specific DNA labeling approach for interaction studies of the nucleosome, we focused on the binding of aclarubicin (aclacynomycin A, short form 'acla', see

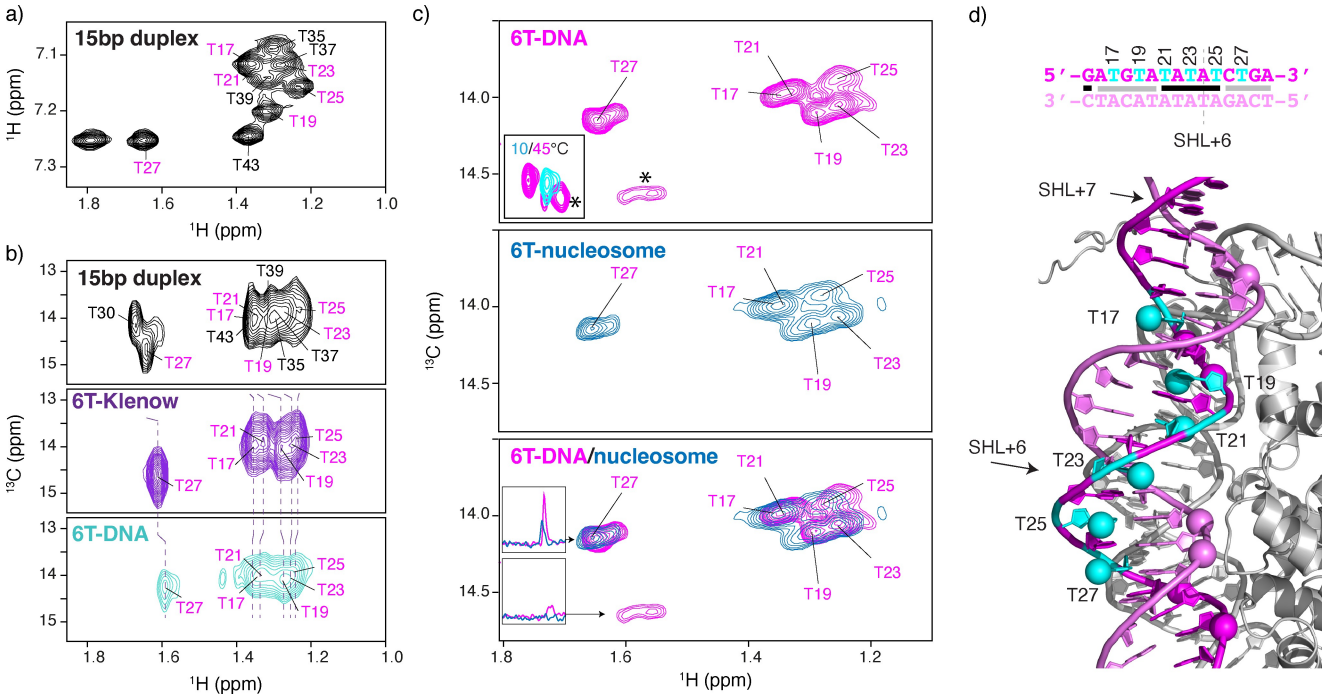

Figure 3. NMR assignment and methyl spectra of 6T-labeled DNA and nucleosomes. (a) Section of 2D ^{1}H-^{1}H NOESY, recorded at 10 °C, showing H6-H7 thymidine correlations in the unlabeled 15 bp duplex. See Figure S2 for sequential assignment. Thymidines that are isotope-labeled in the 6T-DNA (T17 to T27) are highlighted in magenta. (b) Methyl region of the 2D ^{1}H-^{13}C HMQC of the unlabeled 15 bp duplex (top), the 6T-labeled Klenow reaction product (middle), and the 167 bp 6T-labeled DNA (bottom). All spectra recorded at 10 °C. Dashed lines indicate the assignment transfer between conditions. (c) Methyl region of the constant-time HMQC of 6T-labeled 601-DNA (magenta, top) and nucleosome (blue, middle) and their overlay (bottom), recorded at 45 °C, including transferred assignments. The inset in the top panel shows the T27 methyl resonances in HMQC spectra at 10 and 45 °C, see also Figure S3. The minor peak of T27 is marked with an asterisk. The inset in the bottom panel shows the 1D traces through the major and minor peak of T27 for comparison. (d) Location and numbering of the labeled nucleotides T17-T27 (cyan, methyl group shows as a cyan sphere) around SHL 6 of the nucleosome with the DNA sequence shown on top. The black/gray lines indicate regions where the major/minor groove faces the histone octamer. The histone binding platforms are indicated by showing the phosphorus atom as a sphere.

Figure 4a). Using a careful, stepwise procedure up to 6 equivalents of aclarubicin were added to 6T-labeled nucleosomes while preserving nucleosome integrity. This resulted in a significant intensity loss for all methyl peaks except for T27, without clear changes in chemical shift (Figure 4b,c). As intercalation of acla in any of the labeled base pair steps could

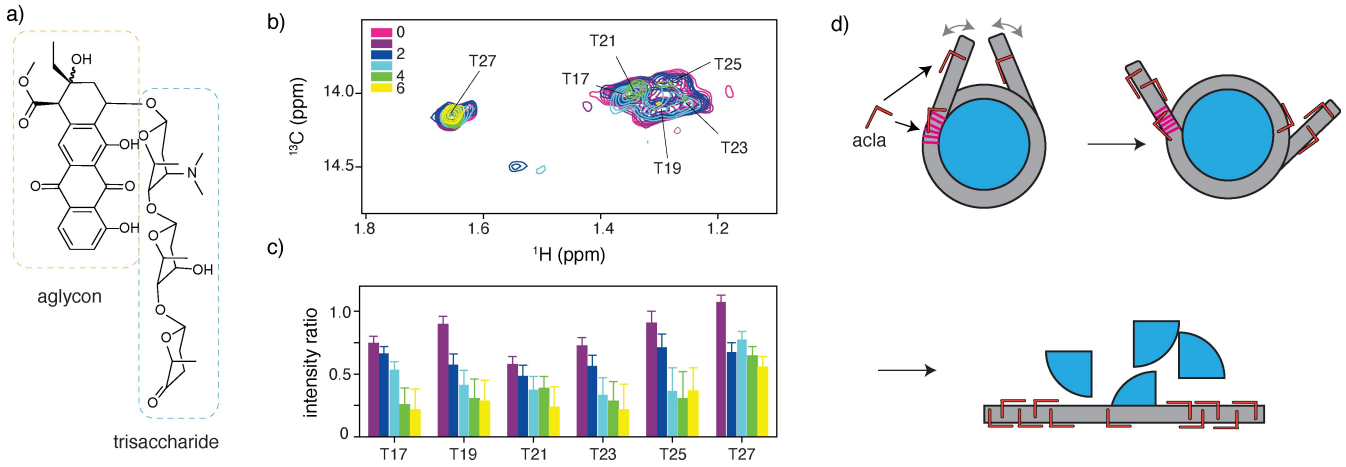

Figure 4. Interaction with aclarubicin (acla). (a) Molecular structure of acla with the intercalating aglycon moiety and the trisaccharide indicated. (b) Methyl region of the constant-time 2D ^{1}H,^{13}C HMQC of 6T-labeled nucleosomes in presence of 0, 1, 2, 3, 4 and 6 equivalents of acla. Color coding indicated. (c) Bar plot showing for each methyl group the intensity ratios of the corresponding peak in presence of acla compared to the free state using the color coding of panel (b). (d) Model of the acla-nucleosome interaction. Acla can bind and intercalate into the linker DNA where the minor groove is fully exposed, and the DNA is not constrained or can bind nucleosomal DNA where only the outward facing minor groove is exposed, and the DNA conformation is constrained by histone-DNA contacts. Transient 'breathing' of the nucleosomal DNA will allow acla to progressively bind more internal sites ultimately resulting in histone eviction.

be expected to induce significant chemical shift changes due to the aromatic ring current effect, these observations suggest that binding of acla can only be visualized indirectly through the disappearance of the free state signals. Close proximity of acla protons, in combination with DNA rigidification and/or increase in μs-ms motions in the bound state, will cause excessive line broadening preventing direct observation of the bound state.

Still, two striking observations can be made. First, addition of 1 equivalent acla affects mostly the peak intensity of T21 and, to a slight lesser extent, T17 and T23 (Figure 4c). Assuming acla will first bind to exposed minor grooves in the nucleosome, there are 14 binding sites in the nucleosome core (1 per turn) and 2 additional binding sites in each of the two linker DNA arms (total 18 binding sites). The observed drop in intensity is much larger than expected from a purely statistical distribution. Interestingly, T21 and T23 are part of the only AT-repeat region in the 601 sequence (see supplementary Scheme S1). This region at SHL 6 also has a solvent-exposed minor groove (see also Figure 3d) and is thus available for binding. Moreover, since histone-DNA contacts in this region are weaker compared to the more internal sites, DNA deformation by intercalation of acla may be accommodated here. It is also conceivable that initial association of acla here may be driven by favorable interactions of the sugars with the AT-minor groove[15] without intercalation. Thus, the effects observed for T21 and T23 are consistent with the reported sequence preference of acla. The effect on T17, the most terminal nucleotide, suggests that, in addition, acla binds first the terminal ends.

Second, at 6 equivalents added, the most inward located methyl, T27 at SHL 5.5, is still mostly unaffected while all other methyl signals have all severely reduced intensities. This suggests that the next minor groove at SHL+5 is not yet occupied by acla, which matches quantitatively with acla being bound in the linker arms (2 per arm) and at SHL +/−6. Our data thus point to a model where aclarubicin initially intercalates in free linker DNA, and any exposed AT-rich minor grooves, and then progressively inwards into the nucleosomal DNA (Figure 4d). Intercalation into linker and terminal (SHL 6,7) DNA is likely energetically more favorable than at internal sites, due to the resulting DNA stretching and unwinding.[34] This will be less well accommodated in regions where the DNA is heavily constrained by the histone-DNA contacts. Initial terminal intercalation may also enhance transient, partial DNA unwrapping thus exposing more DNA for binding and allowing invasion of the DNA by the drug, ultimately resulting in unfolding of the nucleosome and eviction of histones.

We expect that the approach outlined here will be useful in the study of other small molecules or proteins that bind the nucleosome, as well as other protein-DNA complexes involving long stretches of DNA. We expect that uniform labeling used here will be well suited for site-specific solid-state NMR studies. The solution NMR data presented here demonstrate the feasibility of obtaining high-resolution spectra with protonated DNA and deuterated histones. However, to fully benefit from the methyl-TROSY effect in solution, one would need deuterated DNA with specific ^{1}H-^{13}C methyl labeling. While fully deuterated nucleotides are commercially available, specifically methyl-labeled and deuterated thymidine is not, thus requiring custom synthesis. In that case, deuteration of histones is likely not required and deuteration may be restricted to the segment produced during the Klenow fill-in reaction.

Here, we specifically labeled nucleotides at SHL 6 of the nucleosome using a DNA construct that also includes one turn linker DNA at each end. Using the minimal 145 bp nucleosomal DNA, nucleotides in the region from SHL ±7 to SHL ±4 can be labeled in a similar manner. To specifically label nucleotides in SHL 0 to ±3, one would need to produce first a shorter DNA segment with the labeled nucleotides near the end, and then ligate the remainder to obtain the complete nucleosomal DNA.

The divide-and-conquer strategy for resonance assignment used here relies on the structural similarity between the short DNA segment, here the 15 bp duplex, and the larger DNA construct. For many complexes, resonances may be transferred to the complex using titration experiments. For the nucleosome such transfer from free to bound DNA is not possible and thus relies again structural similarity. In case extensive DNA distortion in the bound state would preclude such analysis, the labeling may be tuned to one residue at a time to obtain assignments.

Conclusions

We present a PCR-based method to specifically label nucleosomal DNA for NMR studies, which can be tailored to specific DNA locations and nucleotides of choice. We described the successful incorporation of uniformly ^{13}C-labeled thymidine nucleotides around SHL+6 of the 167 bp 601-DNA sequence and showed that this can be used to probe site-specific effects in the context of the nucleosome.

Our results highlighted the intrinsic conformational heterogeneity at SHL 5.5 in the 601-DNA sequence. We further demonstrated the use of the specifically labeled DNA in an interaction study with anti-cancer drug aclarubicin. We observed that aclarubicin can bind the exposed AT-rich minor groove at SHL 6 and suggest that the drug invades nucleosomes from the terminal ends inward, eventually resulting in histone eviction. These data may explain how anthracyclines induce histone eviction and how the specificity of this process may be manipulated for the targeting of other DNA regions currently untouched by these effective cancer drugs.[35] Overall, the method opens up new opportunities to study the structural dynamics of nucleosomal DNA as function of protein or drug binding.

Supporting Information

The authors have cited additional references within the Supporting Information.[36,37]

Acknowledgements

H.v.I thanks dr. Tammo Diercks (CiC bioGUNE, Bilbao) for sharing his constant-time HMQC pulse sequence. This work was supported by a VIDI grant from the Dutch Science Foundation NWO to HvI (NWO-CW VIDI 723.013.010) and National Roadmap grant 184.032.207 to uNMR-NL, the National Roadmap Large-Scale NMR Facility of the Netherlands.

Conflict of Interests

J.N. is a shareholder in NIHM that aims to produce aclarubicin for clinical use

Data Availability Statement

The data that support the findings of this study are available from the corresponding author upon reasonable request.

Keywords: nucleosome · DNA · NMR · conformation · aclarubicin

[1] K. Zhou, G. Gaullier, K. Luger, *Nat. Struct. Mol. Biol.* **2019**, *26*, 3–13.
[2] G. Li, J. Widom, *Nat. Struct. Mol. Biol.* **2004**, *11*, 763–769.
[3] A. K. Shaytan, G. A. Armeev, A. Goncearenco, V. B. Zhurkin, D. Landsman, A. R. Panchenko, *J. Mol. Biol.* **2016**, *428*, 221–237.
[4] A. Stützer, S. Liokatis, A. Kiesel, D. Schwarzer, R. Sprangers, J. Söding, P. Selenko, W. Fischle, *Mol. Cell* **2016**, *61*, 247–259.
[5] S. O. Dodonova, F. Zhu, C. Dienemann, J. Taipale, P. Cramer, *Nature* **2020**, *580*, 669–672.
[6] K. K. Sinha, J. D. Gross, G. J. Narlikar, *Science* **2017**, *355*, eaaa3761.
[7] Y. Lorch, R. D. Kornberg, B. Maier-Davis, *Proc. Nat. Acad. Sci.* **2023**, *120*, e2216611120.
[8] B. Pang, X. Qiao, L. Janssen, A. Velds, T. Groothuis, R. Kerkhoven, M. Nieuwland, H. Ovaa, S. Rottenberg, O. van Tellingen, J. Janssen, P. Huijgens, W. Zwart, J. Neefjes, *Nat. Commun.* **2013**, *4*, 1908.
[9] B. Pang, J. de Jong, X. Qiao, L. F. A. Wessels, J. Neefjes, *Nat. Chem. Biol.* **2015**, *11*, 472–480.
[10] X. Qiao, S. Y. van der Zanden, D. P. A. Wander, D. M. Borràs, J.-Y. Song, X. Li, S. van Duikeren, N. van Gils, A. Rutten, T. van Herwaarden, O. van Tellingen, E. Giacomelli, M. Bellin, V. Orlova, L. G. J. Tertoolen, S. Gerhardt, J. J. Akkermans, J. M. Bakker, C. L. Zuur, B. Pang, A. M. Smits, C. L. Mummery, L. Smit, R. Arens, J. Li, H. S. Overkleeft, J. Neefjes, *Proc. Nat. Acad. Sci.* **2020**, *117*, 15182–15192.
[11] F. Yang, C. J. Kemp, S. Henikoff, *Curr. Biol.* **2013**, *23*, 782–787.
[12] M. Wooten, B. Takushi, K. Ahmad, S. Henikoff, *Sci. Adv.* **2023**, *9*, eadg3257.
[13] D. Yang, A. H.-J. Wang, *Biochemistry* **1994**, *33*, 6595–6604.
[14] S. Takahashi, N. Nagashima, Y. Nishimura, M. Tsuboi, *Chem. Pharm. Bull.* **1986**, *34*, 4494–4499.
[15] G. Cheng, F. Zhang, X. Tan, P. He, Y. Fang, *Chin. J. Chem.* **2008**, *26*, 1089–1095.
[16] H. Fritzsche, U. Wähnert, J. B. Chaires, N. Dattagupta, F. B. Schlessinger, D. M. Crothers, *Biochemistry* **1987**, *26*, 1996–2000.
[17] J. Rinnenthal, J. Buck, J. Ferner, A. Wacker, B. Fürtig, H. Schwalbe, *Acc. Chem. Res.* **2011**, *44*, 1292–1301.
[18] M. L. Ken, R. Roy, A. Geng, L. R. Ganser, A. Manghrani, B. R. Cullen, U. Schulze-Gahmen, D. Herschlag, H. M. Al-Hashimi, *Nature* **2023**, *617*, 835–841.
[19] J. D. Brown, S. Kharytonchyk, I. Chaudry, A. S. Iyer, H. Carter, G. Becker, Y. Desai, L. Glang, S. H. Choi, K. Singh, M. W. Lopresti, M. Orellana, T. Rodriguez, U. Oboh, J. Hijji, F. G. Ghinger, K. Stewart, D. Francis, B. Edwards, P. Chen, D. A. Case, A. Telesnitsky, M. F. Summers, *Science* **2020**, *368*, 413–417.
[20] S. Ma, A. Kotar, I. Hall, S. Grote, S. Rouskin, S. C. Keane, *Proc. Nat. Acad. Sci.* **2023**, *120*, e2300527120.
[21] M. Ahmed, A. Marchanka, T. Carlomagno, *Angew. Chem. Int. Ed.* **2020**, *59*, 6866–6873.
[22] Y. Bai, B.-R. Zhou, *J. Mol. Biol.* **2021**, *433*, 166648.
[23] G. Abramov, A. Velyvis, E. Rennella, L. E. Wong, L. E. Kay, *Proc. Nat. Acad. Sci.* **2020**, *117*, 12836–12846.
[24] D. W. Conroy, Y. Xu, H. Shi, N. Gonzalez Salguero, R. N. Purusottam, M. D. Shannon, H. M. Al-Hashimi, C. P. Jaroniec, *Proc. Nat. Acad. Sci.* **2022**, *119*, e2200681119.
[25] V. Tugarinov, P. M. Hwang, J. E. Ollerenshaw, L. E. Kay, *J. Am. Chem. Soc.* **2003**, *125*, 10420–10428.
[26] F. H. T. Nelissen, M. Tessari, S. S. Wijmenga, H. A. Heus, *Prog. Nucl. Magn. Reson. Spectrosc.* **2016**, *96*, 89–108.
[27] J. M. Louis, R. G. Martin, G. M. Clore, A. M. Gronenborn, *J. Biol. Chem.* **1998**, *273*, 2374–2378.
[28] F. H. T. Nelissen, F. C. Girard, M. Tessari, H. A. Heus, S. S. Wijmenga, *Nucleic Acids Res.* **2009**, *37*, e114–e114.
[29] P. T. Lowary, J. Widom, *J. Mol. Biol.* **1998**, *276*, 19–42.
[30] C. L. van Emmerik, I. Gachulincova, V. R. Lobbia, M. A. Daniëls, H. A. Heus, A. Soufi, F. H. T. Nelissen, H. van Ingen, *Anal. Biochem.* **2020**, *588*, 113469.
[31] C. Altona, D. H. Faber, A. J. Hoekzema, *Magn. Reson. Chem.* **2000**, *38*, 95–107.
[32] D. Vasudevan, E. Y. D. Chua, C. A. Davey, *J. Mol. Biol.* **2010**, *403*, 1–10.
[33] E. Y. D. Chua, D. Vasudevan, G. E. Davey, B. Wu, C. A. Davey, *Nucleic Acids Res.* **2012**, *40*, 6338–6352.
[34] G. J. Quigley, A. H. Wang, G. Ughetto, G. van der Marel, J. H. van Boom, A. Rich, *Proc. Nat. Acad. Sci.* **1980**, *77*, 7204–7208.
[35] D. P. A. Wander, S. Y. van der Zanden, G. A. van der Marel, H. S. Overkleeft, J. Neefjes, J. D. C. Codée, *J. Med. Chem.* **2020**, *63*, 12814–12829.
[36] F. Delaglio, S. Grzesiek, GeertenW. Vuister, G. Zhu, J. Pfeifer, A. Bax, *J. Biomol. NMR* **1995**, *6*, DOI 10.1007/BF00197809.
[37] W. Lee, M. Tonelli, J. L. Markley, *Bioinformatics* **2015**, *31*, 1325–1327.

Manuscript received: February 4, 2024
Revised manuscript received: March 3, 2024
Accepted manuscript online: March 12, 2024
Version of record online: March 28, 2024